JAMES | Journal of Advances in Modeling Earth Systems

RESEARCH ARTICLE
10.1029/2019MS001679

Key Points:
- Estimates of annual canopy maintenance respiration, a globally important C flux, vary widely among models calibrated from leaf trait data
- Using an optimization framework, we show that the canopy properties maximizing C export depend strongly on the respiration model used
- Leaf-scale empirical models should be applied cautiously at the canopy-scale, particularly in Earth system models with canopy optimization.

Correspondence to:
R. Q. Thomas and M. Williams,
rqthomas@vt.edu;
mat.williams@ed.ac.uk

Citation:
Thomas, R. Q., Williams, M., Cavaleri, M. A., Exbrayat, J.-F., Smallman, T. L., & Street, L. E. (2019). Alternate trait-based leaf respiration schemes evaluated at ecosystem-scale through carbon optimization modeling and canopy property data. *Journal of Advances in Modeling Earth Systems*, *11*, 4629–4644. https://doi.org/10.1029/2019MS001679

Received 5 MAR 2019
Accepted 7 DEC 2019
Accepted article online 10 DEC 2019
Published online 25 DEC 2019

Alternate Trait-Based Leaf Respiration Schemes Evaluated at Ecosystem-Scale Through Carbon Optimization Modeling and Canopy Property Data

R.Q. Thomas[1], M. Williams[2,3], M.A. Cavaleri[4], J.-F. Exbrayat[2,3], T.L. Smallman[2,3], and L.E. Street[2]

[1]Department of Forest Resources and Environmental Conservation, Virginia Tech, Blacksburg, VA, USA, [2]School of GeoSciences, University of Edinburgh, Edinburgh, UK, [3]National Centre for Earth Observation, University of Edinburgh, Edinburgh, UK, [4]School of Forest Resources & Environmental Science, Michigan Technological University, Houghton, MI, USA

Abstract Leaf maintenance respiration ($R_{leaf,m}$) is a major but poorly understood component of the terrestrial carbon cycle (C). Earth systems models (ESMs) use simple sub-models relating $R_{leaf,m}$ to leaf traits, applied at canopy scale. $R_{leaf,m}$ models vary depending on which leaf N traits they incorporate (e.g., mass or area based) and the form of relationship (linear or nonlinear). To simulate vegetation responses to global change, some ESMs include ecological optimization to identify canopy structures that maximize net C accumulation. However, the implications for optimization of using alternate leaf-scale empirical $R_{leaf,m}$ models are undetermined. Here we combine alternate well-known empirical models of $R_{leaf,m}$ with a process model of canopy photosynthesis. We quantify how net canopy exports of C vary with leaf area index (LAI) and total canopy N (TCN). Using data from tropical and arctic canopies, we show that estimates of canopy $R_{leaf,m}$ vary widely among the three models. Using an optimization framework, we show that the LAI and TCN values maximizing C export depends strongly on the $R_{leaf,m}$ model used. No single model could match observed arctic and tropical LAI-TCN patterns with predictions of optimal LAI-TCN. We recommend caution in using leaf-scale empirical models for components of ESMs at canopy-scale. $R_{leaf,m}$ models may produce reasonable results for a specified LAI, but, due to their varied representations of $R_{leaf,m}$foliar N sensitivity, are associated with different and potentially unrealistic optimization dynamics at canopy scale. We recommend ESMs to be evaluated using response surfaces of canopy C export in LAI-TCN space to understand and mitigate these risks.

Plain Language Summary While we have good understanding of plant photosynthesis, its links to climate and leaf nitrogen and process models to estimate photosynthesis; the same is not true for respiration. Measurements of leaf respiration are used to calibrate simple respiration models, which are applied at canopy-scale. Here we investigate the risks associated with using various alternate simple respiration models in the context of viewing plant canopies as economic structures that must produce more carbon through photosynthesis than they use in respiration and tissue construction. We model the carbon economy of canopies with measured properties (leaf coverage and nitrogen) in arctic and in the tropical ecosystems, comparing the results using three different respiration models. First, we note the respiration estimates vary greatly among the models, so the models are not consistent. Second, we show that the optimal canopy properties (those most economically successful) also depend strongly on the respiration model used. This means that the choice of respiration model will have significant effects on the predictions of canopy response, and therefore C cycling, under global change. Our research highlights the need for more robust, process modeling of respiration.

1. Introduction

Respiration by leaves (R_{leaf}) is a major component of the global carbon (C) cycle. R_{leaf} is linked to foliar metabolism for the maintenance of leaf function ($R_{leaf,m}$) and for leaf construction ($R_{leaf,g}$). R_{leaf} has been estimated to comprise ~50% of total autotrophic respiration, which is the largest contribution of any plant tissue (Atkin et al., 2007), and represents ~30-Gt C released globally by terrestrial ecosystems per year (Atkin et al., 2017), a flux much larger than current fossil fuel emissions. At the ecosystem system, R_{leaf}

has been estimated to account for 43% of total (vegetation and soils) respiration in a tropical forest (Cavaleri et al., 2017), greater than any other component (soils, live wood, and woody debris). Therefore, predicting the dynamics of R_{leaf} across biomes is critical for simulating current and future global C cycling. While detailed and robust biochemical models of photosynthesis exist that are applied globally (Farquhar & von Caemmerer, 1982), an equivalent for leaf maintenance respiration is lacking.

In lieu of mechanistic models of $R_{leaf,m}$, Earth system models (ESM) that simulate global C cycling use empirical $R_{leaf,m}$ models that are derived from the analysis of leaf trait databases. Observations of $R_{leaf,m}$ come largely from direct, instantaneous measurements at the leaf scale (Field et al., 1982). Cuvettes clamped to leaves can measure net photosynthesis and $R_{leaf,m}$ from darkening the cuvette. Sampling provides information on $R_{leaf,m}$ variation across space (i.e., climate), leaf chemistry, species, and time (Atkin et al., 2015; Heskel et al., 2016). For global simulations, leaf trait data are used to parametrize $R_{leaf,m}$ models designed to scale from the leaf to the canopy for different plant functional types (Bonan et al., 2012; Xu et al., 2017). This scaling is performed using submodels that simulate $R_{leaf,m}$ at the leaf scale with the simple empirical functions before being summed to the canopy based on leaf area index (LAI) or leaf mass. This scaling process is an ongoing challenge because we largely lack direct measurements of integrated $R_{leaf,m}$ at canopy scale (but see Wehr et al., 2016). Therefore, it is important to evaluate the sensitivities of canopy scale flux predictions to assumptions about the leaf-to-canopy scaling, particularly in ESMs models designed to simulate C—climate feedbacks across the globe.

ESMs are increasingly including ideas of optimality and competition in their representations of C cycling. For example, dynamic vegetation models aim to predict how different plant strategies, including allocation, traits, and structure of canopies, affect competition among plants and ecosystem C dynamics (Fisher et al., 2018; Moorcroft et al., 2001). These models rely on leaf trait data on metabolism (e.g., respiration) and structure (e.g., N concentration; Wright et al., 2004) to inform their parameters. The increased use of optimality concepts in ESMs builds on a long-standing impetus to link leaf traits to economic theories of optimal canopy or plant-scale states and function (Bloom et al., 1985) and to ecosystem fluxes and properties (Reichstein et al., 2014). Optimization concepts in models provide a framework to link environmental conditions and resources to canopy processes and properties in order to create more robust canopy models (Fisher et al., 2015). With optimization as a guide, economic models aim to predict the climate sensitivity of canopy processes and canopy properties, both critical requirements for ESMs. Optimal canopy properties are those which maximize the export of C after other costs are paid (McMurtrie & Dewar, 2011). The key properties are LAI and TCN, which are closely linked to photosynthesis via light absorbing area (LAI) and Rubisco concentration (TCN) and to respiration via maintenance of metabolic capacity (TCN) and growth respiration associated with production of leaves (LAI). Both LAI and TCN arise from the contributing population of leaves and leaf-level traits, including N content, leaf mass per area (LMA), and leaf lifespan. Overall, $R_{leaf,m}$ is a major component of the interaction of key canopy processes (photosynthesis, allocation, and respiration) that determine the optimal canopy structure (LAI and TCN). However, the empirical models of $R_{leaf,m}$ that have been used in the simulation of leaf and canopy respiration differ in their complexity (i.e., number of parameters and covariates) and empirical form (i.e., linear vs. nonlinear)—thus requiring further investigation into how the form of $R_{leaf,m}$ influences predictions of canopy processes and structure.

Here we tested how three alternate, well-known empirical $R_{leaf,m}$ models (Atkin et al., 2017; Reich et al., 2008; Ryan, 1991), influence canopy respiration and optimal LAI and TCN predictions. The three respiration models are seemingly similar because they are all constructed from databases of leaf traits and predict $R_{leaf,m}$ as a function of foliar nitrogen. However, they differ in whether the relationship is between foliar N concentration or TCN, whether the relationship is linear or nonlinear, and whether additional covariates are included (i.e., climate). First, we characterize how predictions of total leaf respiration from these three models vary when scaled to the canopy. Second, we analyze how the three $R_{leaf,m}$ models influence predictions of canopy C budgets and optimal canopy structure and therefore competitive outcomes at the ecosystem scale. We hypothesize that using a more complex $R_{leaf,m}$ model (i.e., more parameters and covariates) will lead to closer agreement between predicted optimal canopy properties and field observations of canopies because the additional covariates represent more variation in the global leaf trait data used in the empirical fitting. To test the hypothesis, we analyzed the economics of the canopy carbon balance and optimal canopy

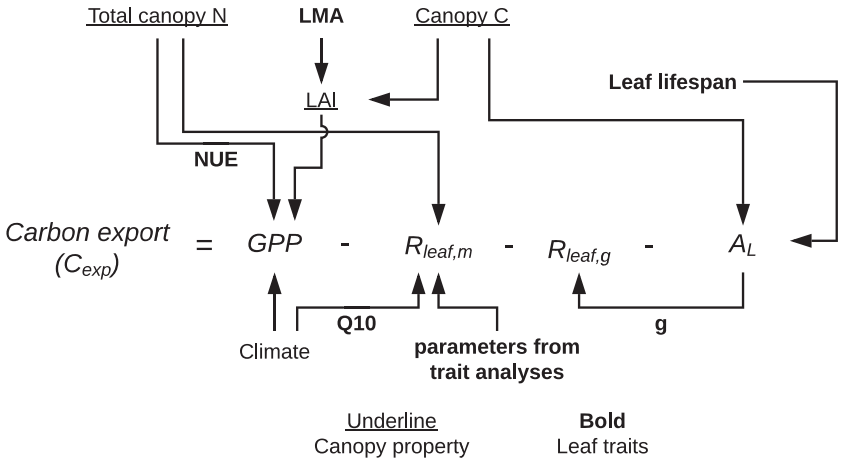

Figure 1. The canopy carbon balance equation and its inputs, shown here, defines the canopy carbon economy. The equation determines how the mass of carbon exported from the canopy (C_{exp}) is derived from canopy properties (underlined), climate, and leaf traits (**bold**). Gross primary production (GPP), maintenance and growth respiration ($R_{leaf,m}$, $R_{leaf,g}$), and the C cost of investment (leaf allocation, A_L) are the canopy processes that govern how the canopy properties, climate, and leaf traits alter canopy carbon export. Leaf traits include leaf mass per area (LMA), leaf lifespan, and parameters ($R_{leaf,m}$ model specific) that control the response of maintenance respiration to canopy properties. NUE, Q_{10}, and g are parameters that govern the response of photosynthesis to canopy N, the response of $R_{leaf,m}$ to temperature, and the proportion of A_L used for growth respiration, respectively.

properties (LAI and TCN) using a single model for photosynthesis, allocation, and leaf turnover coupled to the three alternate empirical models of $R_{leaf,m}$.

Our analysis focused on three canopy types in two different biomes where direct (destructive) measurements of LAI and TCN and associated leaf traits are available. Two of the canopy types are low arctic shrubs—one deciduous and one evergreen—from Alaska. The third canopy type is tropical rainforest composed of broadleaf evergreen trees in Costa Rica. Thus, we are able to evaluate the variation in canopy economics and optimal canopy properties across a major climate gradient and across the leaf economic spectrum related to leaf lifespan (deciduous vs. evergreen) against robust leaf and canopy data.

2. Methods

To assess the consistency of the three different $R_{leaf,m}$ models at canopy scale, we constructed a simple canopy-scale carbon balance model. This model represents photosynthesis, allocation, and respiration (each of the three alternate $R_{leaf,m}$ can be selected), including their relationships with canopy N and environmental conditions. We then use the carbon balance model to calculate marginal returns on canopy C and N investment and predict optimal canopy properties, varying the $R_{leaf,m}$ submodel, to address the questions above.

2.1. Model Description

We simulate the net canopy C export over annual cycles (C_{exp}, g C m^{-2} yr^{-1}) as the critical optimization variable for canopy economics (McMurtrie & Dewar, 2011). The model takes account of photosynthetic uptake, fixed structural costs, and variable metabolic costs (Figure 1):

$$C_{exp} = GPP - R_{leaf,m} - R_{leaf,g} - A_L, \quad (1)$$

where GPP is gross photosynthesis, $R_{leaf,m}$ is canopy maintenance respiration, $R_{leaf,g}$ is canopy growth respiration, and A_L is the allocation of primary production to foliage (all g C m^{-2} yr^{-1}). The model runs for 1 year at the daily time-step using meteorology, LAI, TCN, and parameters described below as inputs. All analyses focus on the annual sums of the fluxes in equation (1).

2.1.1. GPP Model

We derived estimates of GPP by emulating a multilayer canopy model, Soil-Plant-Atmosphere (SPA; Williams et al., 1996). The SPA model uses detailed photosynthesis equations (Farquhar & von

Caemmerer, 1982) and tracks radiative transfer and leaf level energy balance. The key model drivers are physical (temperature, vapor pressure deficit, and daily solar radiation) and biological (LAI) and (TCN). For the tropical simulations, the optimum temperature for electron transport and Ribulose 1,5-bisphosphate (RuBP) regeneration was set to 30°C (Williams et al., 1998). For the arctic simulation, the optima were set to 20°C (Williams et al., 2000), because of known differences in photosynthetic temperature optima (Kumarathunge et al., 2019). We assumed a well-developed root system and well-watered soil (i.e., total soil-to-atmosphere hydraulic resistance was not limiting photosynthesis), so the simulations are valid when soil moisture is close to field capacity at some point in the rooting profile. Therefore, we restrict our analysis to sites where the assumption of sufficient soil moisture for photosynthesis generally applies. Canopies were set up with four canopy layers, each with the same leaf area density (25% of LAI in each layer). Total canopy N was distributed with an approximately exponential decline from canopy top (40% in top layer, 25% in layer 2, 20% in layer 3, to 15% in the lowest layer). A ~twofold change in leaf N per area from well-lit to shaded leaves is consistent with the results of a global analysis of within-canopy trait data (Niinemets et al., 2015).

Because exploration of optimal allocation of plant resources required numerous simulations of GPP at different combinations of LAI and TCN, we calibrated the aggregated canopy model (Williams et al., 1997) to emulate SPA across a global range of drivers following Smallman and Williams (2019). The equations used in the aggregated canopy model and the methods used to construct the emulator can be found in the supporting information.

2.1.2. $R_{leaf,m}$ Models

Carbon losses from maintenance respiration ($R_{leaf,m}$) have been linked to functions of air temperature and foliar N (Atkin et al., 2015; Reich et al., 2008; Ryan, 1991), but the exact shape, whether a linear or power function, remains uncertain. To allow for flexibility in the relationship between leaf N and maintenance respiration and to allow for the use of parameters from global analyses of leaf respiration, we used three different formations of $R_{leaf,m}$. The first form is from Ryan (1991) and has been used in ESMs (i.e., community land model versions 4.0 and 4.5; Oleson et al., 2010; Oleson et al., 2013). It linearly scales canopy respiration with TCN using a single slope parameter:

$$R_{leaf,m(\mathrm{Ryan},20)} = m_1 \times \mathrm{TCN} \tag{2}$$

where m_1 is a parameter. The reference temperature is 20°C.

The second form is from a global analysis of leaf respiration provided by Atkin et al. (2015), which is used in the Community Land Model version 5.0 (Lawrence et al., 2019). It linearly estimates respiration based on area-based leaf nitrogen concentrations and temperature using three parameters:

$$R_{\mathrm{leaf,m(Atkin},25)} = (m_2 + m_3 N_a - m_4 TWQ)\ \mathrm{LAI} \tag{3}$$

where m_2, m_3, and m_4 are parameters, N_a is the N content per unit leaf area, TWQ is the temperature of the warmest three consecutive months of the year, and LAI is the leaf area index. The reference temperature is 25°C. By including a temperature adjustment to the respiration at a baseline temperature (the m_4 parameter), this model represents the acclimation of respiration rates to local climate (TWQ).

Finally, the third form is from a global analyses of leaf respiration (Reich et al., 2008) that uses nitrogen per leaf mass (N_m, g N g leaf biomass^{-1}) as the key leaf trait. It nonlinearly estimates respiration based on mass-based leaf nitrogen concentrations:

$$R_{\mathrm{leaf,m(Reich},20)} = 10^{m_5 + m_6 log10(N_m)} (\mathrm{LAI} \times \mathrm{LMA} \times 2.0) \tag{4}$$

where m_5 and m_6 are parameters and the term in the second parentheses converts LAI to canopy biomass because the respiration is on a mass basis (hence the carbon to biomass conversion of 2.0). Equation (4) is in log10 form to directly use the parameters from the log10-log10 fit reported in Reich et al. (2008). The reference temperature is 20°C.

To scale from the reference temperature to the daily maintenance respiration, we used a Q_{10} value of 2 to govern the temperature sensitivity, $f(T)$. All canopy types had the same Q_{10} function (the factor by which

Table 1
Climatic Conditions During the Growing Season and Leaf Traits for the Three Canopy Types in Two Different Biomes Used to Evaluate the Canopy Optimization Model

Canopy type	Temp (° C)	Radiation (MJ day^{-1})	Season (days)	LMA (g C m^{-2})	Leaf lifespan (days)	Leaf growth start (day of year[a])	First day of leaf drop (day of year[a])	Mean LAI (range)
Arctic deciduous	10.2	16.3	90	41	90	160	260	1.32 (0.10–4.16)
Arctic evergreen	10.2	16.3	90	85	800	160	260	0.50 (0.07–1.04)
Tropical evergreen	26.5	14.8	365	44	440	N/A	N/A	6.03 (1.2–12.94)

Note. Note C units for LMA. Leaf area index (LAI) mean and range from in situ data are shown.
Abbreviations: LAI, leaf area index; LMA, leaf mass per area.
[a]January 1 is the first day-of-year.

respiration increases for every 10°C rise in temperature), consistent with how temperature sensitivity is often represented in ESMs (i.e., the Community Land Model)

2.1.3. $R_{leaf,g}$ and A_L and Models

C losses from growth respiration ($R_{leaf,g}$) were a constant proportion (g) of A_L ($R_{leaf,g} = g\,A_L$). Our estimates of A_L assumed a canopy at steady-state; therefore, annual A_L was equal to the annual turnover of C in leaves. For leaf lifespans <1 year (i.e., deciduous), annual A_L and turnover were equal to the maximum leaf C associated with the specified LAI and LMA. For leaf lifespans >1 year, annual A_L and turnover were defined as the maximum leaf C divided by the leaf lifespan. For example, a 300 g C m^{-2} maximum leaf C with a leaf lifespan of 3 years required 100 g C m^{-2} of A_L to occur in the spring.

Seasonal phenology was simulated by initiating allocation at a specified leaf-on day of year (Table 1) and adding a constant fraction of A_L daily over a specified number of days (20 days for deciduous, 60 days for evergreen). The seasonal phenology applied to both the arctic deciduous and evergreen canopy types, with the evergreen adding foliage to the existing canopy during the growing season. Litterfall occurred after a specified day of year (Table 1) and was equal to A_L, equally spread over a specified number of days (20 days for deciduous and 120 days for evergreen). Growing season is defined as the difference between the day of year for the initiation of leaf growth and day of year for the initiation of leaf drop. Tropical evergreen phenology was simulated by setting the leaf C equal to the maximum leaf C throughout the year but requiring A_L (and litterfall) to be equal to that required to maintain the canopy for a given leaf lifespan. The growing season length was a full year for the tropical evergreen canopy.

2.2. Calculation of Optimal Canopy Properties

We calculated optimal canopy properties using two different numerical approaches. First, we simulated the annual fluxes for each of the components of equation (1) using a range of LAI and TCN values and examined the response surfaces that describe each flux on LAI and TCN axes. Then, using each flux at each LAI-TCN combination, we solved equation (1) to develop a response surface describing how C_{exp} varies with LAI and TCN.

Second, based on economic principles, plants should invest in their canopies to provide positive net returns (i.e., income exceeds investment). By calculating the canopy properties that are consistent with such principles, we generated an estimate of optimal canopy structure for specific leaf traits and climate. To achieve this, we determined the marginal returns of C investment across LAI-TCN phase space by making small adjustments to foliar C (∂C) at each LAI-TCN combination and calculating the impact on C_{exp} over a full annual cycle (365 days), in an adjustment to equation (1):

$$\frac{\partial C_{exp}}{\partial \mathrm{Leaf}_C} = \left(\sum_{i=1}^{365} \frac{\partial \mathrm{GPP}_i}{\partial \mathrm{Leaf}_C} - \sum_{i=1}^{365} \frac{\partial R_{\mathrm{leaf,m}_i}}{\partial \mathrm{Leaf}_C}\right) - \frac{\frac{\partial \mathrm{Leaf}_C}{\mathrm{LL}}}{\partial \mathrm{Leaf}_C} - \frac{\frac{\partial \mathrm{Leaf}_C \times g}{\mathrm{LL}}}{\partial \mathrm{Leaf}_C} \quad (5)$$

Because the additional C ($\partial \mathrm{Leaf}_C$) persists for the leaf-life span, the allocation term (third on the right-hand side of equation (5)) and growth respiration term (fourth term on the right-hand side of equation (5)) were divided by the leaf lifespan (LL) if LL > 1 year.

We calculated the annual marginal return of C for N investment by adding a small amount of N ($\partial \mathrm{Leaf_N}$) at each LAI-TCN combination to calculate changes in C_{exp}. The marginal return reflects the dependence of GPP on TCN and $R_{\mathrm{leaf,m}}$ on N_a. Because the focus is on the export of C, the allocation of N was not included in the marginal calculation.

$$\frac{\partial C_{\mathrm{exp}}}{\partial \mathrm{Leaf}_N} = \left(\sum_{i=1}^{365} \frac{\partial \mathrm{GPP}_i}{\partial \mathrm{Leaf}_N} - \sum_{i=1}^{365} \frac{\partial \mathrm{R}_{\mathrm{leaf,m}\ i}}{\partial \mathrm{Leaf}_N} \right) \tag{6}$$

We numerically solved equations (5) and (6) at range of specified LAI and TCN values to generate a response surface of $\frac{\partial C_{\mathrm{exp}}}{\partial \mathrm{Leaf}_C}$ and $\frac{\partial C_{\mathrm{exp}}}{\partial \mathrm{Leaf}_N}$ in LAI-TCN phase space.

2.3. Site Descriptions and Observational Data

Canopy types are defined and differentiated by their climate (e.g., temperature, growing season length, and solar radiation) and leaf traits of dominant vegetation (e.g., LMA and LL). We parameterized and applied the models for three canopy types (two arctic and one tropical), each with data on local leaf traits, canopy properties, and climate (Table 1). The evergreen tropical canopy type was a moist tropical rainforest recorded at La Selva Biological Station in Costa Rica (elevation 37–150 m, 10°20′N, 83°50′W; Clark et al., 2008). The two low-stature arctic canopy types were recorded at Toolik Lake (Williams & Rastetter, 1999) on the north slope of Alaska (elevation 930 m, 68°37′N 149°18′W). These three canopies allow comparison between tropic and arctic climates and across the LES fast-slow gradient (deciduous versus evergreen shrub tundra canopies).

Each field site had observations of LAI and TCN that we used to simulate canopy fluxes and to evaluate model predictions of optimal and optimizing canopy properties across variation in climate and leaf traits (Cavaleri et al., 2010; Street et al., 2012). The observations were direct measurements of LAI and TCN for the three canopy types, where all leaves were destructively harvested from the top of the canopy to the ground throughout a vertical column. The area of all the leaves within each column and their N content were used directly to calculate the vertically integrated LAI and TCN, and mean LMA. The complete harvesting approach avoids the uncertainties associated with limited sampling at various heights or layers in the canopy. Direct harvesting correctly weights the variation of leaf traits through the vertical profile.

For the tropical canopies at La Selva, the average height for the old growth forest was 20 m, with some emergent trees from 30–60 m. The canopy was sampled in columns at 45 locations, each accessed with a walk-up scaffolding tower. Towers were randomly located in mature forest to include variation in the degree of canopy closure (Clark et al., 2008). The area of the column sampled at each tower was 4.56 $\mathrm{m^2}$. Leaves from the entire profile were collected, sorted into five functional groups, dried, and weighed. A functional group subsample from each 2-m height range was measured for LMA (g $\mathrm{m^{-2}}$) and mass-based foliar nitrogen (%N), thus resolving vertical variation in traits. From these data, we determined LAI or TCN by combining the height profiles of leaf mass with LMA or %N.

For the arctic canopies at Toolik Lake, we used observations where entire canopies of shrubs were harvested by clipping all leaves within the volume over 0.04 $\mathrm{m^2}$ quadrats (Van Wijk et al., 2005; Williams & Rastetter, 1999). Sampled foliage was divided by species then dried and weighed. A species subsample was measured for leaf area to determine LMA and then also for %N. The sampled canopy columns in the arctic survey were characterized as deciduous shrubs (*Salix* spp, *Betula nana*, and *Vaccinium uliginosum*, $n = 32$) or evergreen shrubs (*Ledum palustre*, *Empetrum nigrum*, and *Vaccinium vitis-idaea*, $n = 29$) by species dominance. We determined canopy LAI or TCN by scaling the total sampled dry leaf mass of each species with its LMA or %N measurements and summing for all species.

2.4. Model Simulations and Analysis

Our model simulations focused on evaluating the sensitivity of maintenance respiration predictions to the underlying respiration-N relationship and on exploring how this relationship influences canopy export and optimization of canopy properties. We undertook the following simulations for all three canopy types, spanning the LES from slow to fast leaves and from arctic to tropical climates:

1. We predicted total annual maintenance respiration at the observed LAI-TCN combinations for each canopy type to explore the sensitivity of maintenance respiration to the three respiration models.

2. We modeled the response surface of GPP, $R_{leaf,m}$, A_L, and $R_{leaf,g}$ across a full potential range of LAI and TCN. A unique response surface was calculated for each of the three canopy types and for each maintenance respiration model. These simulations provide context for the optimization modeling.
3. We combined the GPP, $R_{leaf,m}$, A_L, and $R_{leaf,g}$ response surfaces to calculate net canopy C export (equation (1)) for each of the three canopy types and respiration models to locate and explain the C_{exp} maxima in LAI-TCN phase space. By calculating the response surface of C_{exp} to variations in LAI-TCN and $R_{leaf,m}$ model, the approach identifies TCN-LAI combinations that are nonviable (e.g., negative C_{exp}).
4. We calculated the marginal change in C_{exp} associated with a small investment in either canopy leaf C ($\partial Leaf_C$) or leaf N ($\partial Leaf_N$) relative to a given LAI (LAI/LMA) and TCN value in the LAI-TCN phase space. Using the marginal calculations, we determined the values of LAI and TCN with positive marginal returns on investment for both C and N (i.e., equations (5) and (6) are both positive). The value of LAI-TCN with positive marginal returns is likely a subset of the values of LAI-TCN where C_{exp} is positive and defines optimal canopy properties.

Model simulations used daily weather data from meteorological stations at La Selva and Toolik Lake (year 2007 data for both sites). The parameters for LMA, LL, leaf out, and leaf fall day were site- and canopy-specific based on observations at the site or plant trait databases (Table 1). Growth respiration was a fixed fraction ($g = 0.28$) of A_L (Waring & Schlesinger, 1985). We used reported values for each of the respiration parameters: $m_1 = 0.0106$ (Ryan, 1991; Figure 1); $m_2 = 1.7560$, $m_3 = 0.2061$, and $m_4 = 0.0402$ (Atkin et al., 2015; supporting information, Table S4 ESM #2 absolute form); $m_5 = 0.691$ and $m_6 = 1.639$ (Reich et al., 2008; Table 1 All Leaves).

3. Results and Discussion

3.1. Influence of Leaf-Scale $R_{leaf,m}$ Model on Canopy Carbon Fluxes

3.1.1. Patterns in Canopy Respiration Across Observed LAI and TCN for Differing Leaf Respiration Models

The three $R_{leaf,m}$ models have clear differences in their response surfaces when visualized in LAI-TCN phase spaces (Figure 2). The Ryan model (Figures 2a, 2d, and 2g) is sensitive only to TCN, being entirely determined by total canopy N content and insensitive to its concentration. Therefore, the N sensitivity is linear to increasing TCN under all combinations of LAI and TCN. The Atkin model (Figures 2b, 2e, and 2h) is sensitive to both TCN and LAI, responding linearly to changes in both of these properties. The Reich model (Figures 2c, 2f, and 2i) is also sensitive to both LAI and TCN, but responds nonlinearly, with the largest changes in respiration per change in TCN occurring at higher levels of TCN.

Simulations based on in situ observations of LAI, TCN, and meteorological drivers revealed major differences in predictions of annual, canopy-scale $R_{leaf,m}$ (Figure 3). In all cases, the Ryan model tended to generate lower $R_{leaf,m}$ estimates, on average 33–71% less than other models (depending on canopy type and model). The Ryan model also had the lowest spread in $R_{leaf,m}$ across measured ranges in canopy properties. In the tropics, Reich and Atkin models produced similar peak $R_{leaf,m}$ estimates, but Reich had the greatest $R_{leaf,m}$ for those canopies with high TCN (Figure 2).

These results show how these three models, using different empirical relationships to relate leaf N to $R_{leaf,m}$, produce contrasting outcomes when applied at canopy scale. Therefore, naïve use of the $R_{leaf,m}$ models in C cycle models can have potentially important implications for the vegetation C balance. We describe how this variation has important implications for how C cycling is optimized in each biome in section 3.2

3.1.2. Predicted Components of Annual Canopy Carbon Budget Across Observed LAI and TCN

$R_{leaf,m}$ is a component of the canopy C balance that also includes photosynthesis (GPP), leaf allocation (A_L), and growth respiration ($R_{leaf,g}$). Photosynthesis is maximized by a balance between LAI and TCN; a limitation to either of these leads to strong constraint on GPP (Figure 4). The underlying photosynthesis model we used predicts C uptake on the basis of light absorption and area for gas exchange, both correlated to LAI; and on the carboxylation potential, which is correlated with TCN. These factors have typical nonlinear responses that interact to create a strong gradient with GPP maximized at high LAI and TCN for each canopy type. The degree of saturation of GPP with increasing LAI-TCN (i.e., the increasing distance between contour lines in Figure 4) is clearest in the tropical canopy types. $R_{leaf,g}$ and A_L have similar response surfaces in LAI-TCN space, being determined only by allocation to C, not N (Figure 4). The allocation of C to leaves is similar

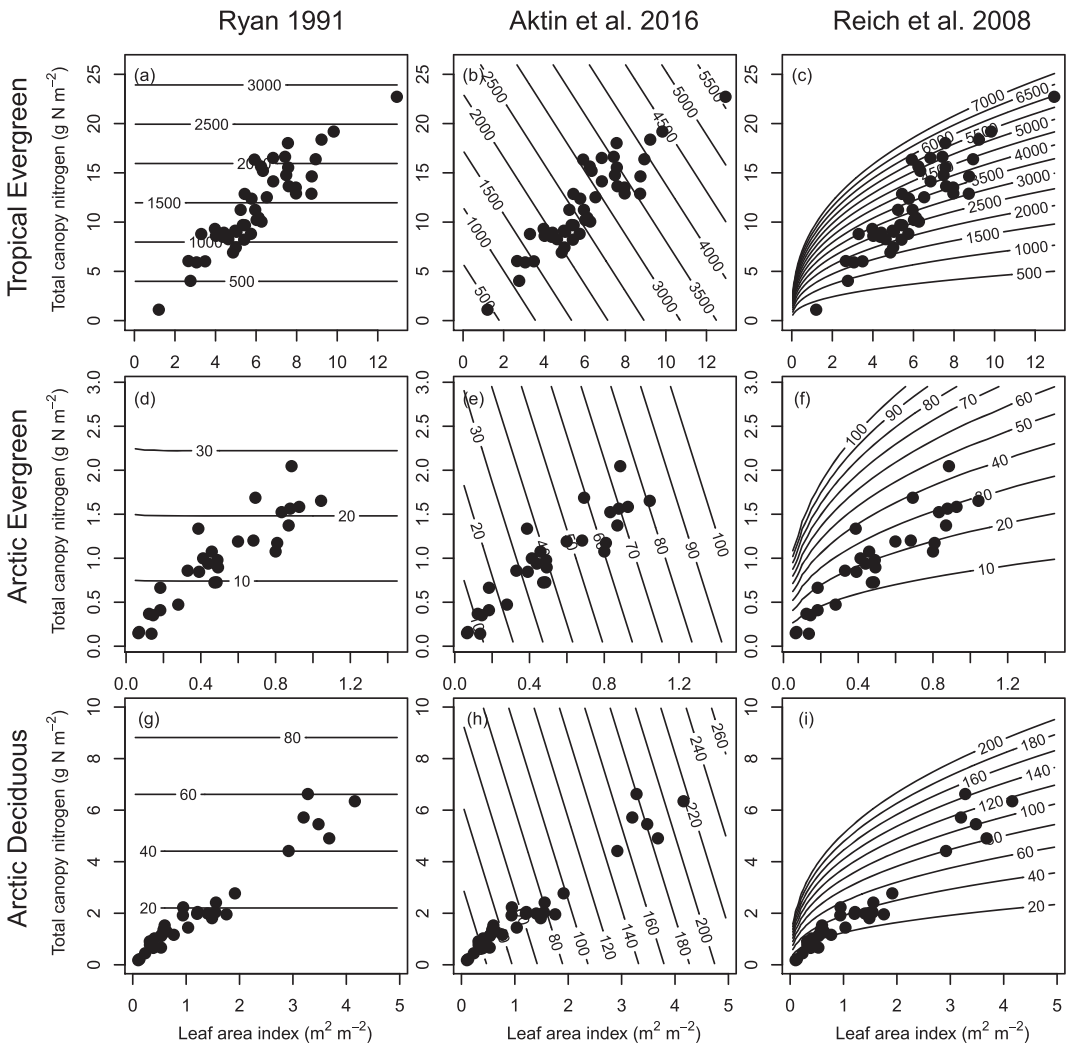

Figure 2. Variation in annual maintenance respiration ($R_{\text{leaf, m}}$) across LAI-TCN phase space for three different canopy types (rows show tropical evergreen, arctic evergreen, and arctic deciduous canopies) as estimated using three different $R_{\text{leaf, m}}$ models: column 1 is from equation (2), column 2 is from equation (3), and column 3 is from equation (4) in the text. Contours are annual sum of $R_{\text{leaf, m}}$ for the canopy in units of g C m^{-2} yr^{-1}. Symbols show the LAI and TCN combinations from the three field sites; the values of the contours at these points indicate the expected range of $R_{\text{leaf, m}}$ for each respiration model at these LAI and TCN values.

between the three canopy types, despite differences in parameterized LL and LMA (Table 1), due to the correlation between the two traits: the short-lived deciduous canopy had lower mass per leaf area, resulting in similar allocation, for a given LAI, to the arctic evergreen canopy with more mass per leaf area. $R_{\text{leaf,g}}$ is parameterized to be a constant proportion of A_{L}. As a result, there is a simple linear increase in $R_{\text{leaf,g}}$ and A_{L} with increasing LAI that does not depend on TCN.

Observed canopy LAI-TCN combinations broadly ascend an optimal "ridge" in LAI-TCN space for photosynthesis (Figure 4). The GPP predicted at the observed LAI-TCN for the three canopy types generated an order of magnitude variation in predicted photosynthesis between tropics and arctic, consistent with a similar span in TCN and LAI. The co-development of LAI and TCN shown in the data (i.e. maintenance of a similar LAI-TCN ratio across canopies) supports the hypothesized development of canopies that maximize GPP, as indicated by the optimal ridge in the response surface.

Across canopy types, climate differences lead to greater GPP in the tropics compared to arctic vegetation at the same LAI, while A_{L} and $R_{\text{leaf,g}}$ show no such variation (Figure 4). For similar LAI-TCN, GPP is ~three-fold larger in the tropics compared to arctic deciduous canopy type under local climate conditions. For

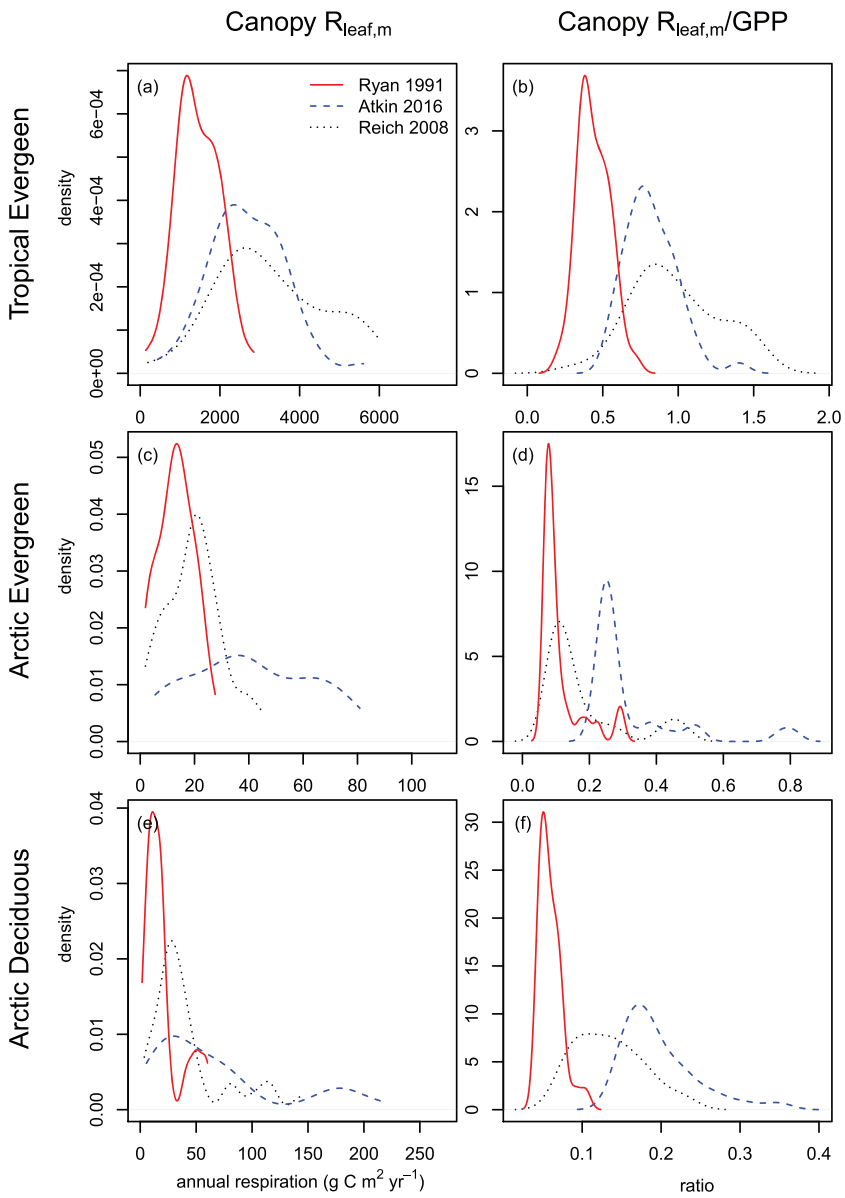

Figure 3. The density distribution of canopy maintenance respiration ($R_{leaf,m}$; panels a, c, and e) and the ratio of $R_{leaf,m}$ to gross photosynthesis (GPP; panels b, d, and f) as estimated using the three different $R_{leaf,m}$ models, for three different canopy types (one for each panel), using observed data on LAI and TCN as inputs. The distribution of the observed LAI-TCN is shown as dots in Figure 2.

similar LAI-TCN, both $R_{leaf,g}$ and A_L in the tropics are similar compared to arctic deciduous canopy type. $R_{leaf,g}$ and A_L have costs associated only with C investment and have no climate sensitivity.

The ratio of $R_{leaf,m}$: GPP is highly variable across $R_{leaf,m}$ models and canopy types (Figure 3). The Ryan model has consistently lower ratios for each canopy type. The Reich model is highest for the tropics, and the Atkin model is highest for the two arctic canopy types. In the tropical case, the Reich and Atkin estimates are unrealistically large, with ratios close to 1. In such cases, canopy export is unlikely to be positive, and hence, the canopy C cycle is not competitive or even viable. In the arctic canopy types, the model ratios are consistently lower, but still variable across the models.

These results show that the climate sensitivity of the $R_{leaf,m}$ models is much larger than the GPP model. The pattern of $R_{leaf,m}$: GPP for observed canopy types (Figure 3 right panels) is similar in pattern to the $R_{leaf,m}$ distributions (Figure 3 left panels), and the differences between models and across canopy types are

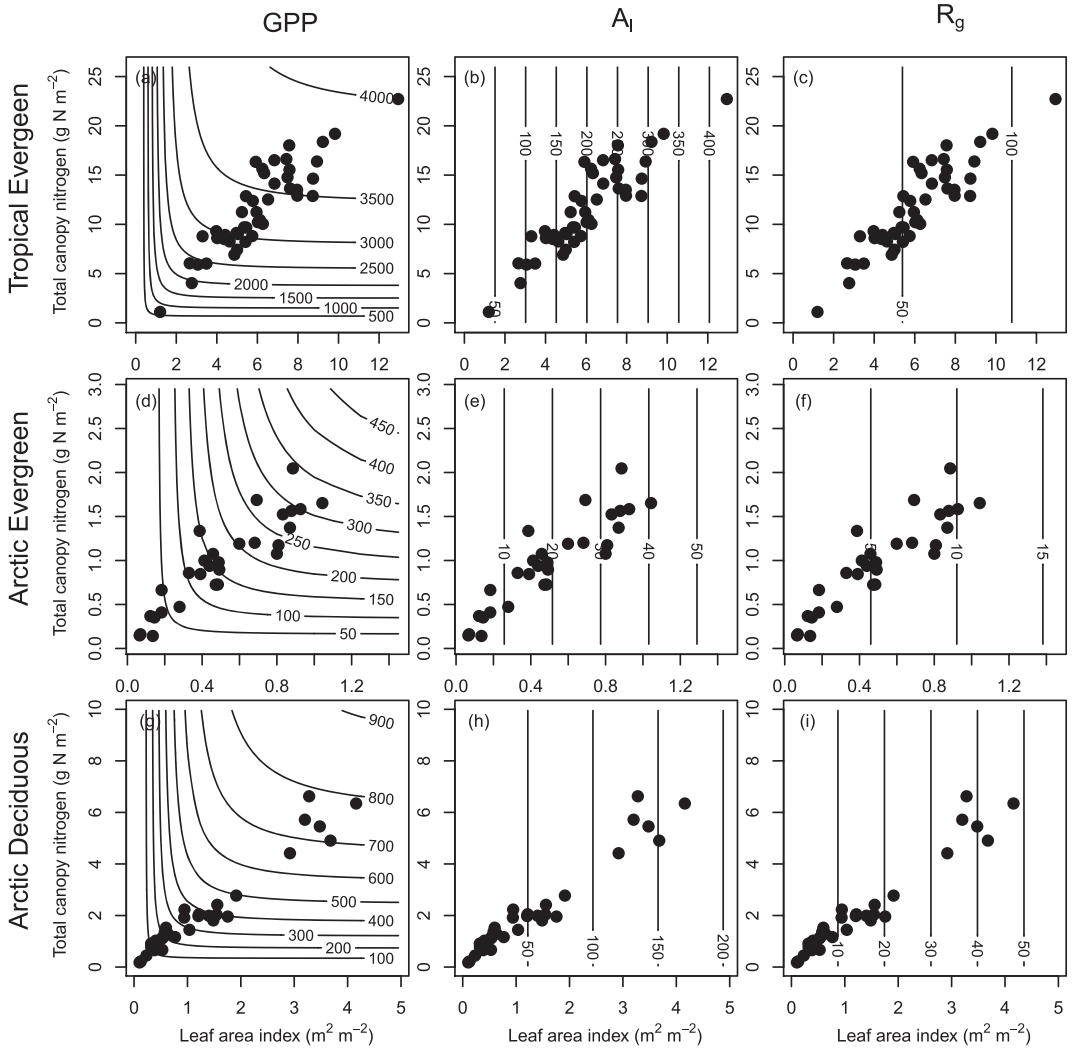

Figure 4. Variation in annual gross photosynthesis (GPP), leaf allocation (A_L), and growth respiration ($R_{leaf,\ g}$) across canopy phase space for three different canopy types (rows show tropical evergreen, arctic evergreen, and arctic deciduous examples) as estimated by specific models for each process (columns). Contours are the annual sum of GPP, A_L, and $R_{leaf,\ g}$ in units of g C m^{-2} yr^{-1}. Symbols show the LAI and TCN combinations for observed canopies at the two field sites in the Arctic and one in the tropics; the values of the contours at these points indicate the expected annual rate for each process at realistic combinations of LAI and TCN.

significant in the context of overall C budgets. This variation in GPP and $R_{leaf,m}$ across canopy types and $R_{leaf,\ m}$ models will influence optimization of the carbon available for export from the canopy (C_{exp}), which is discussed in section 3.2.

3.1.3. The Balance Between Canopy Photosynthesis and Respiration in Models and Observations

An analysis of canopy scale field-based estimates of photosynthesis and leaf respiration from both arctic and tropical canopies suggests a broad consistency in their relative magnitudes. Cavaleri et al. (2017) estimated a mean canopy photosynthesis (GPP estimated from the MAESTRA model) of 4,290-g C m^{-2} yr^{-1} for the tropical forest site used here, and using chamber measurements of components of ecosystem respiration estimated a mean R_{leaf} of 1,540-g C m^{-2} yr^{-1}, with a R_{leaf} : GPP ratio of 0.36. López-Blanco et al. (2017) studied a mixed (deciduous and evergreen) shrub tundra in Greenland, combining flux measurements and modeling to estimate a mean canopy photosynthesis of 148-g C m^{-2} yr^{-1}, a mean R_{leaf} of 47-g C m^{-2} yr^{-1}, with a R_{leaf}: GPP ratio of 0.32. R_{leaf} is the combined growth ($R_{leaf,g}$) and maintenance respiration ($R_{leaf,m}$).

These values of R_{leaf}: GPP derived from upscaled field observations of fluxes are inconsistent with the estimates from the model outputs of this study (Figure 3). For the tropics, the mean ratios derived were 0.84

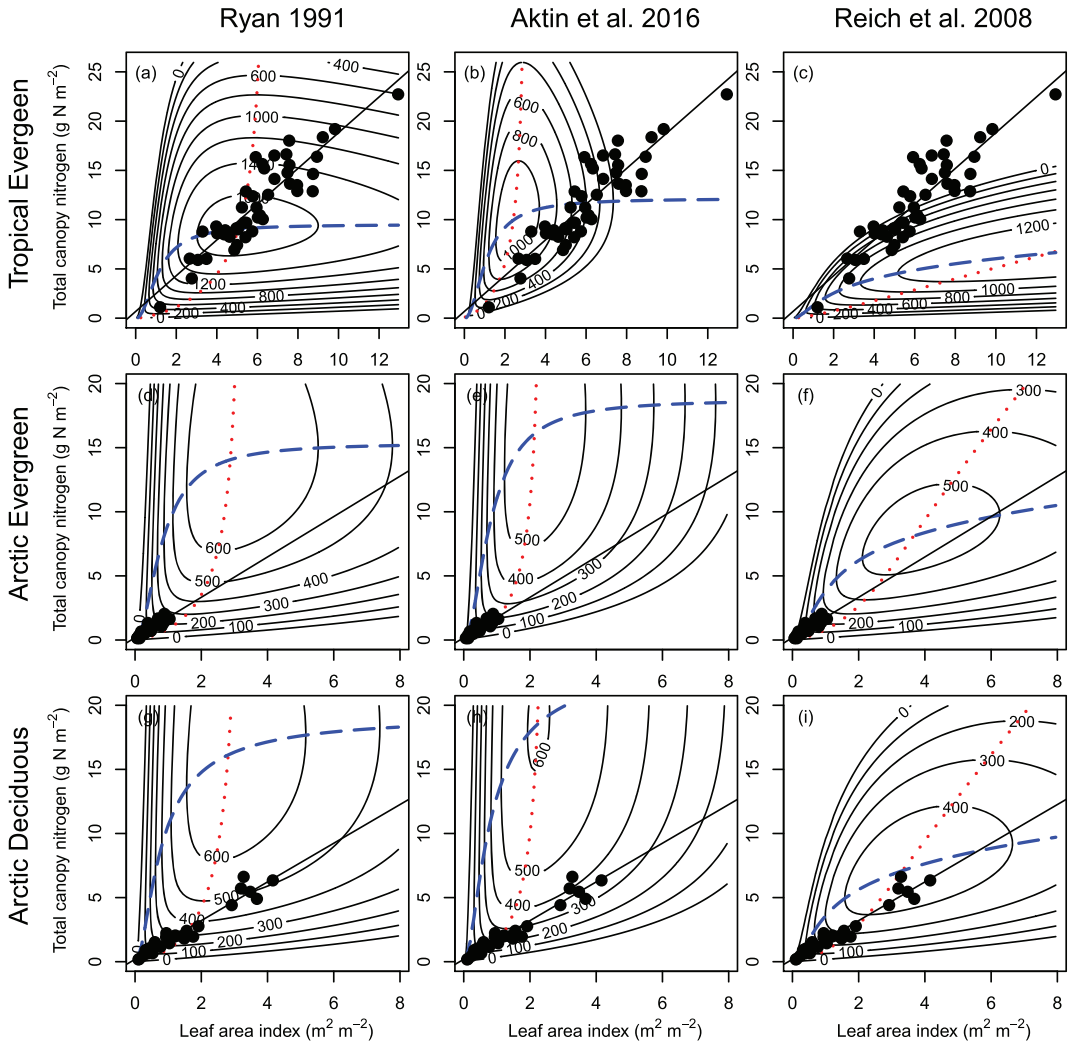

Figure 5. Variation in annual net canopy C export (C_{exp}) across canopy phase space for three different canopy types (rows show tropical evergreen, arctic evergreen, arctic deciduous examples) as estimated using equation (1) with three different $R_{leaf,\ m}$ models. The calculation of C_{exp} used the values for GPP, A_L, and $R_{leaf,\ g}$ from Figure 4 and $R_{leaf,\ m}$ from Figure 2 at the range of LAI-TCN combinations in the figures. Contours are C_{exp} in units of g C m^{-2} yr^{-1}. Symbols show the observed LAI and TCN collected at the three field sites; the values of the contours at these points indicate the expected range of C_{exp} at realistic LAI-TCN combinations using the three different respiration models. The red dotted and blue dashed lines are the marginal threshold curves of carbon export determined via analytical calculations delimiting positive marginal returns on investment into N (blue dashed) and carbon (red dotted, carbon is related to LAI). The marginal threshold curves define the areas of phase space which will result in positive or negative returns on investment. Only in the area that is both below the blue dashed curves and above the red dashed curve will there be positive returns on both N and C investment. The optimal canopy, which maximize C export, is indicated by the non-zero point where the two curves intersect. The black line shows the regression through the LAI-TCN data.

(Atkin), 0.46 (Ryan), and 1.0 (Reich). For the evergreen shrub tundra, the mean ratios were 0.36 (Atkin), 0.15 (Ryan), and 0.22 (Reich). And for the deciduous shrub, the mean ratios derived were 0.24 (Atkin), 0.10 (Ryan), and 0.18 (Reich). In all these comparisons, the modeled ratios are poorly related to the independent data estimates (apart from Atkin $R_{leaf,m}$ for evergreen tundra).

3.2. Influence of Leaf-Scale $R_{leaf,m}$ Model on Predictions of Optimal Canopy Structure

3.2.1. Net Canopy Export is Maximized at Specific LAI and TCN

For all models and canopy types, there is a clear optimum for C_{exp} in LAI-TCN phase space (Figure 5). The C_{exp} response surface is determined as the net of the GPP, $R_{leaf,m}$, $R_{leaf,g}$, and A_L response surfaces (Figures 2 and 4) by equation (1). The contour plots show C_{exp} rising consistently from the origin to a peak value, as

increasing LAI and TCN generate positive net returns on investment. At higher values of LAI and TCN, C_{exp} declines from its peak, as the costs of maintaining high LAI and TCN exceed the gains in photosynthesis. Photosynthesis has a strong saturating response, particularly at the high values of LAI and TCN found in the tropics (Figure 4), whereas the costs from $R_{leaf,g}$ (Figure 4) and A_L do not saturate.

The optimum C_{exp} is also directly indicated by the intersection of marginal thresholds for C and N allocation (shown by the dashed lines in Figure 5). The intersection indicates the point beyond which any further allocation of N and/or C will lead to net reduction in C_{exp}. This is exactly consistent with the contour plotting on the same figures, indicating the robustness of the economic calculations independently made here (equation (1) vs. equations (5) and (6)). From the optimum C_{exp}, we can identify the optimum LAI and TCN that maximize C_{exp}. For canopy properties below these optima, the marginal thresholds define those combinations of LAI and TCN that are remunerative, that is, a lens-shaped region where additions of either N or C lead to net gains in C_{exp}. This region is determined by the positive zone of marginal responses for C (to the left of the red dotted line) and N (below the blue dashed line).

While there is a single optimal pairing of LAI and TCN that maximizes C export, there are multiple viable leaf trait pathways towards this optimum within the marginal thresholds. Previous explorations of optimization in Dewar (1996), Franklin and Ågren (2002), and McMurtrie and Dewar (2011) are all broadly consistent with our mapping. Both linear and nonlinear trajectories in how TCN optimally responds to variations in LAI (and vice versa) are viable. Canopies can develop with mean leaf traits changing as canopies close (increasing LAI); this situation matches the proposed N addition threshold to the optimizing domain (blue line). In these non-N limiting situations, our optimization shows that canopies can develop initially with investment preferentially into TCN over LAI, using the C returns to ultimately invest in LAI and achieve optimality. Canopies can also develop as Franklin and Ågren (2002) suggest, with a consistent LAI-TCN, so that mean leaf traits do not vary with canopy closure; this situation affords the strongest marginal returns overall, by increasing net C export at or close to the steepest possible gradient. Our analysis further shows how strongly N-limited canopies could optimize by investing initially in LAI, following the lower, C addition threshold of the optimizing domain (red dotted line).

3.2.2. Optimal Canopies for Net C Export

There is little consistency in the optimal canopy properties generated by the three $R_{leaf,m}$ models for each canopy type (Figure 5). Differences in $R_{leaf,m}$ models influence predictions of optimal canopy structure and therefore competitive outcomes at ecosystem scale. The Atkin optimum tropical canopy has LAI = 2.5, TCN = 10.1. The Reich optimum canopy has LAI = 12.8, TCN = 6.7. For comparison, in the tropics the Ryan model has an optimum canopy LAI = 5.1, TCN = 9.1. For arctic evergreen canopies, Ryan and Atkin models produce similar optimal canopy properties, LAI = 2.2–2.9, TCN = 14.1–16.2, suggesting high leaf N concentration (TCN/LAI). The Reich model has an optimum with LAI = 3.7, TCN = 8.2 and thus much lower leaf N concentration. For arctic deciduous canopies the pattern is similar to the evergreen analysis. Atkin and Ryan models predict similar optima, with lower LAI and higher TCN than the Reich model. The variation in leaf traits between fast (deciduous) and slow (evergreen) has little impact on the economics of the canopies at the arctic site. The high LMA, long lived (high LL) traits for the evergreen canopy trade-off similarly with the low LMA, low LL leaf traits of the deciduous shrubs. There is no obvious interaction of leaf traits like LL and LMA with the $R_{leaf,m}$ models (Figure 2).

The economic modeling identifies combinations of canopy properties that have negative net export (Figure 5) Thus, we can isolate economically nonviable canopies in phase space. The Ryan model is associated with the broadest range of viable canopies, with the $C_{exp} > 0$ threshold extending across most of the phase space explored for all canopy types (i.e., positive contour lines are throughout LAI-TCN space in Figure 5). The reasons for the different behavior in C_{exp} among $R_{leaf,m}$ models can be directly traced to the response surfaces of the $R_{leaf,m}$ models (Figure 2) and their relationships to C gain, GPP (Figure 4). The Ryan model tends to have the lowest ratios of $R_{leaf,m}$: GPP (Figure 3), which means the C remaining for export is greater than the other $R_{leaf,m}$ models. Hence using Ryan $R_{leaf,m}$ leads to a much large viable set of LAI-TCN combinations in the economic calculations. Atkin and Reich have similar $R_{leaf,m}$: GPP ratios, but very different viable canopy properties due to the differences in how LAI and TCN interact to determine $R_{leaf,m}$. The strongly nonlinear response of the Reich $R_{leaf,m}$ model to increasing TCN means that low TCN canopies are more viable. The steeper response of GPP to TCN variation in the tropics

(Figure 4) linked to the $R_{leaf,m}$ response of the Atkin model to mean high TCN; low LAI canopies are more viable.

In the tropics, the viable canopy phase space is much smaller for Atkin and Reich models, but the viable spaces mapped by these two models are nearly completely distinct. The Atkin $R_{leaf,m}$ model suggests that economically viable tropical canopies will tend to high TCN and lower LAI. The Reich $R_{leaf,m}$ model suggests the opposite pattern, with competitive (i.e., high C_{exp}) tropical canopies tending to higher LAI and lower TCN. The trends are similar, but less extreme for arctic canopies. The Atkin $R_{leaf,m}$ model leads to broader viable coverage of LAI-TCN phase space than in the tropics, but still tends towards higher TCN canopies being more viable. Reich $R_{leaf,m}$ has a more symmetrical pattern of viable canopies, with no clear tendency towards LAI or TCN dominating viability. Again, the arctic canopies do not show differences in economies depending on LL, showing little sensitivity to coupled variation in LMA and LL.

3.2.3. Net Canopy Export of Observed Versus Predicted Optimal

In many cases, in situ observations of canopy properties do not match the theorized optimum canopy properties or the economically viable areas within C_{exp} canopy phase space (Figure 5). We make the comparison between data and theory in two ways, to test our hypothesis that a more complex $R_{leaf,m}$ model should produce more consistent matches of optimal canopy properties to observations. First, we evaluate whether the data points sit within the economically viable space identified by the marginal threshold curves. Second, we test whether the slope of the observed relationship between TCN and LAI data bisects the theoretical viable space and intersects the optimal canopy properties.

For the tropical case, each $R_{leaf,m}$ model produces a very different evaluation. The Ryan model outputs match the slope of the observed TCN-LAI well. But the predictions of optimum LAI and TCN using the Ryan model are about half the observed maximum observed LAI and are less than the mean LAI-TCN (Figure 5). Furthermore, many of the in situ data exceed the predicted canopy optima. For predictions using the Atkin model, the mismatch between the model and the data is clear. Nearly all the in situ data are outside the economically viable region of phase space; the predicted optimum is much lower than observed maxima for LAI and TCN, and the observed slope LAI-TCN is much shallower than that predicted. For predictions using the Reich model, the mismatch is also very clear, with the slope of observed LAI-TCN relationship steeper than expected, although the maximum value of LAI predicted is similar to the observed maximum.

For the arctic evergreen canopies, the range of observed LAI and TCN is low (LAI $< <2$). This means that most of the data sit within the economically viable envelopes of the economic modeling (Figure 5). However, for Ryan and Atkin, there is a large mismatch between predicted optimum canopy properties and the slope of LAI-TCN from observations. The modeling suggests the canopy should prioritize investment into N rather than LAI, whereas the data suggest a more balanced allocation. For Reich $R_{leaf,m}$, the slope of the LAI-TCN data is much closer to bisecting the economically viable space from theory. If canopies were to develop along the slope, they would be following an economically viable trajectory.

For arctic deciduous canopies there is a broader range of in situ observations to support the analysis of model consistency ($0 <$ LAI < 5). While the patterns among $R_{leaf,m}$ models are similar to those from the arctic evergreen comparison, there are clearer indications that Ryan and Atkin $R_{leaf,m}$ models estimate a TCN optima that is inconsistent with observations. In both cases, the models suggest very high TCN is optimal, whereas the data support a more conservative relationship for TCN-LAI. For the Reich $R_{leaf,m}$ model, there is closer agreement. The optimum canopy TCN: LAI from the model is a close, though not exact match to the data, and the range of LAI and TCN predicted to be economically viable is broadly consistent with the range of observations.

The analysis of the processes driving net C export suggests that the modeling of temperature sensitivity of the component processes drives the differences in C_{exp} across phase space. We see that the low temperature arctic ecosystems have reduced maintenance respiration costs (Figure 2) relative to the fixed costs of growth respiration and allocation to leaf biomass (Figure 4). This temperature adjustment explains the tendency for optimization to favor higher TCN: LAI ratios (Figure 5) in arctic canopy types compared to the tropical rain forest.

From this visual analysis, we learn that none of the $R_{leaf,m}$ models produced upscaled estimates of respiration that were economically consistent across all the canopy types we investigated, and we reject our hypothesis on model complexity. The models have identifiable strengths and weaknesses. The Ryan model (one parameter) has the least biased estimate of canopy properties for the tropical canopy—it balances the LAI and TCN costs best, although its optimum is lower than the site mean LAI-TCN. The Reich $R_{leaf,m}$ model (two parameters) produced outputs most consistent with data for both arctic canopies. The observed maxima and predicted optima were similar. The Atkin model (three parameters) was weakest overall, with a strong tendency for predicting higher TCN relative to LAI than was ever observed in the data.

3.2.4. How Do We Cope With Variance in Data When Evaluating Optimization?

It is possible to calibrate the parameters each of the $R_{leaf,m}$ models to match the in situ data better (results not shown). However, the calibration process is underdetermined because we cannot isolate the optimum canopy properties from measurements. Indeed, we do not know the correct sampling scale for understanding economic optimization. For example, should the optimum in the tropics be optimized to the maximum observed LAI value (13) or the mean across the samples (6)? The large difference between the mean and maximum observed value could be due to variation in limitations to growth (e.g. competition for light capture or nutrient limitation) that should be captured in the model. However, it could also be an artifact of the spatial scale of sampling, particularly its relation to the size of the organisms and the underlying disturbance regime (Hurtt et al., 2016). Overall, work is needed to identify the correct scale of comparison for model and data and to identify the appropriate spatial scale for accessing the maximum LAI of a canopy within a site.

The basis of our optimization is that a specific arrangement of leaves (represented at canopy scale by LAI-TCN) will maximize canopy C economics. However, the optimization is dependent on exogenous factors, such as climate, soil moisture, and nutrient availability. Our scheme calculates how optimization of C_{exp} varies with mean climate, but we have not explored the effect of interannual variation in climate on optimization, nor long-term climate change effects. We have not explored soil moisture effects; we could implement adjustments to the GPP model to include soil moisture controls on stomatal closure and photosynthesis. Nor have we evaluated soil nutrient effects, as doing so requires a link to root development and activity and would generate more complex economic feedbacks around allocation above and below ground. Likewise, we have not include leaf aging effects in our optimization, for simplicity (Xu et al., 2017).

We suggest that the limitation of observed arctic canopy properties to values below the optima suggested by the model is likely linked to nutrient limitations (i.e., restrictions to TCN). This conclusion is consistent with experimental fertilization studies that have shown that LAI and production for shrubs at Toolik Lake can more than double under N addition (Shaver et al., 2001). However, our results are tentative, because the calculated optimal LAI-TCN is so sensitive to the choice of $R_{leaf,m}$ model and its parameterization. We urgently require process resolving models of leaf metabolism to advance our understanding of C economy of canopies.

3.3. Implications for ESMs

Our analysis clearly maps out the risks in using leaf-trait-based models of plant processes, like $R_{leaf,m}$, within ecosystem C cycle models. Such models are core components of ESMs and drive their biogeochemical cycling. The leaf trait data represent a major community effort, and their analysis provides important insights into links between leaf structure and process. However, upscaling to the canopy scale for implementation within ecosystem models in demonstrably challenging. The leaf trait databases have large variations that are summarized through statistical regression to generate empirical models for hypothesis testing, for example, to examine climate sensitivity or covariation with other leaf traits. However, we show that directly using an empirical form from leaf trait analysis may potentially generate problems in ESMs. The implications of using the empirical forms in ESMs, particularly those that include the optimization of canopy N, should be more closely examined. Transitions between empirical models that use similar covariates, similar to the transition between the Ryan and Atkin models that occurred between the community land model 4.5 and 5.0, could have unintended consequences on the canopy C balance.

Our economic modeling provides a robust a priori framework for evaluating trait-functional parameterizations and hence can transparently link plant trait data sets to ESM calibration and evaluation. We suggest that ecosystem and ESMs should be evaluated using the response surfaces of annual photosynthesis, maintenance respiration, and leaf allocation in LAI-TCN space. This approach will guide understanding of the

implicit trade-offs in the model and compare the domains of inferred optimizing canopies to the LAI-TCN relationships presented here. This need is particularly important for models that include competitive outcomes or allow internal trait adjustment.

4. Conclusions

Leaf-trait data are routinely used to fit various proposed models of leaf respiration for use as components in ESMs. We found that the form of the $R_{leaf,m}$ model leads to markedly different predictions when scaled to the canopy. Thus, $R_{leaf,m}$ model structure plays a more significant role than do databases of leaf trait measurements in determination of canopy C balance and C sequestration in ESMs. Leaf traits, for example, foliar N content, influence both C uptake (photosynthesis) and loss ($R_{leaf,m}$), and these trait-process connections are represented in ESMs. ESMs also link and upscale leaf traits and processes to canopy properties, such as LAI and TCN, thereby coupling C and N cycles. Choice of $R_{leaf,m}$ model influences process–property interactions, particularly affecting the optimal (maximizing C export) properties of a canopy. Examination of how C processing (photosynthesis, $R_{leaf,m}$) varies across LAI, and total canopy N phase space provides insight into process interactions within models. This mapping also shows how optimization in LAI and TCN would proceed to maximize C export. Differences in $R_{leaf,m}$ model structure and parameterization strongly influence predictions of optimal canopy structure and therefore competitive outcomes at ecosystem scale. Our results raise questions about how trait-based models and parameterizations are selected for inclusion in ESMs and for how optimization is included in ESMs. Comparison against observed patterns in LAI and total canopy N presented here are a starting point for ESM diagnosis and for evaluating optimization schemes.

Author Contributions

R.Q. Thomas and M. Williams conceived of the idea, designed the work, created the modeling framework, analyzed simulations, and drafted the text. M.A. Cavaleri and L.E. Street provided data and inputs to analysis and writing. J.-F. Exbrayat and T.L. Smallman contributed to model calibration, analysis, and writing.

Acknowledgments
We acknowledge the financial support of USDA-NIFA McIntire-Stennis Program VA-136633, USDA-NIFA Project #2015-67003-23485, NERC's National Centre for Earth Observation (contract number PR140015), NERC GREENHOUSE project, and the Royal Society. We thank Ed Rastetter and Gus Shaver for their contributions towards generating the arctic data and discussions on optimization. We thank Cayelan Carey for helpful comments on the manuscript. The tropical forest data were collected with support from the US National Science Foundation (ATM-0223284). The data and code used to produce our analysis can be found at www.doi.org/10.5281/zenodo.3530841

References

Atkin, O., Scheurwater, I., & Pons, T. (2007). Respiration as a percentage of daily photosynthesis in whole plants is homeostatic at moderate, but not high, growth temperatures. *New Phytologist*, *174*(2), 367–380. https://doi.org/10.1111/j.1469-8137.2007.02011.x

Atkin, O. K., Bahar, N., Bloomfield, K., Griffin, K. L., Heskel, M. A., Huntingford, C., & de la Torre, A. M. (2017). In G. Tcherkez & J. Ghashghaie (Eds.), *Plant respiration: Metabolic fluxes and carbon balance* (p. 302). Switzerland: Springer.

Atkin, O. K., Bloomfield, K. J., Reich, P. B., Tjoelker, M. G., Asner, G. P., Bonal, D., et al. (2015). Global variability in leaf respiration in relation to climate, plant functional types and leaf traits. *New Phytologist*, *206*(2), 614–636. https://doi.org/10.1111/nph.13253

Bloom, A. J., Chapin, F. S. III, & Mooney, H. A. (1985). Resource limitation in plants—an economic analogy. *Annual Review of Ecology and Systematics*, *16*, 363–392. https://doi.org/10.1146/annurev.es.16.110185.002051

Bonan, G. B., Oleson, K. W., Fisher, R. A., Lasslop, G., & Reichstein, M. (2012). Reconciling leaf physiological traits and canopy flux data: Use of the TRY and FLUXNET databases in the community land model version 4. *Journal of Geophysical Research*, *117*, G02026. https://doi.org/10.1029/2011JG001913

Cavaleri, M. A., Coble, A. P., Ryan, M. G., Bauerle, W. L., Loescher, H. W., & Oberbauer, S. F. (2017). Tropical rainforest carbon sink declines during El Niño as a result of reduced photosynthesis and increased respiration rates. *New Phytologist*, *216*(1), 136–149. https://doi.org/10.1111/nph.14724

Cavaleri, M. A., Oberbauer, S. F., Clark, D. B., Clark, D. A., & Ryan, M. G. (2010). Height is more important than light in determining leaf morphology in a tropical forest. *Ecology*, *91*(6), 1730–1739. https://doi.org/10.1890/09-1326.1

Clark, D. B., Olivas, P. C., Oberbauer, S. F., Clark, D. A., & Ryan, M. G. (2008). First direct landscape-scale measurement of tropical rain forest leaf area index, a key driver of global primary productivity. *Ecology Letters*, *11*(2), 163–172. https://doi.org/10.1111/j.1461-0248.2007.01134.x

Dewar, R. C. (1996). The correlation between plant growth and intercepted radiation: An interpretation in terms of optimal plant nitrogen content. *Annals of Botany*, *78*(1), 125–136. https://doi.org/10.1006/anbo.1996.0104

Farquhar, G. D., & von Caemmerer, S. (1982). In O. L. Lange, P. S. Nobel, C. B. Osmond, & H. Ziegler (Eds.), *Physiological plant ecology II. Encyclopedia of plant physiology (New Series)* (pp. 549–587). Berlin: Springer-Verlag.

Field, C., Berry, J. A., & Mooney, H. A. (1982). A portable system for measuring carbon dioxide and water vapour exchange of leaves. *Plant, Cell and Environment*, *5*, 179–186. https://doi.org/10.1111/1365-3040.ep11571607

Fisher, R. A., Koven, C. D., Anderegg, W. R., Christoffersen, B. O., Dietze, M. C., Farrior, C. E., et al. (2018). Vegetation demographics in Earth system models: A review of progress and priorities. *Global Change Biology*, *24*(1), 35–54. https://doi.org/10.1111/gcb.13910

Fisher, R. A., Muszala, S., Verteinstein, M., Lawrence, P., Xu, C., McDowell, N. G., et al. (2015). Taking off the training wheels: The properties of a dynamic vegetation model without climate envelopes, CLM4.5(ED). *Geoscientific Model Development*, *8*(11), 3593–3619. https://doi.org/10.5194/gmd-8-3593-2015

Franklin, O., & Ågren, G. (2002). Leaf senescence and resorption as mechanisms of maximizing photosynthetic production during canopy development at N limitation. *Functional Ecology*, *16*(6), 727–733. https://doi.org/10.1046/j.1365-2435.2002.00674.x

Heskel, M. A., O'Sullivan, O. S., Reich, P. B., Tjoelker, M. G., Weerasinghe, L. K., Penillard, A., et al. (2016). Convergence in the temperature response of leaf respiration across biomes and plant functional types. *Proceedings of the National Academy of Sciences*, *113*(14), 3832–3837. https://doi.org/10.1073/pnas.1520282113

Hurtt, G. C., Thomas, R. Q., Fisk, J. P., Dubayah, R. O., & Sheldon, S. L. (2016). The impact of fine-scale disturbances on the predictability of vegetation dynamics and carbon flux. *PLoS ONE*, *11*(4). https://doi.org/10.1371/journal.pone.0152883

Kumarathunge, D. P., Medlyn, B. E., Drake, J. E., Tjoelker, M. G., Aspinwall, M. J., Battaglia, M., et al. (2019). Acclimation and adaptation components of the temperature dependence of plant photosynthesis at the global scale. *New Phytologist*, *222*(2), 768–784. https://doi.org/10.1111/nph.15668

Lawrence, D. M., Fisher, R. A., Koven, C. D., Oleson, K. W., Swenson, S. C., Bonan, G., et al. (2019). The Community Land Model version 5: Description of new features, benchmarking, and impact of forcing uncertainty. *Journal of Advances in Modeling Earth Systems*, *11*. https://doi.org/10.1029/2018MS001583

López-Blanco, E., Lund, M., Williams, M., Tamstorf, M. P., Westergaard-Nielsen, A., Exbrayat, J.-F., et al. (2017). Exchange of CO_2 in Arctic tundra: Impacts of meteorological variations and biological disturbance. *Biogeosciences*, *14*(19), 4467–4483. https://doi.org/10.5194/bg-14-4467-2017

McMurtrie, R. E., & Dewar, R. C. (2011). Leaf-trait variation explained by the hypothesis that plants maximize their canopy carbon export over the lifespan of leaves. *Tree Physiology*, *31*(9), 1007–1023. https://doi.org/10.1093/treephys/tpr037

Moorcroft, P. R., Hurtt, G., & Pacala, S. W. (2001). A method for scaling vegetation dynamics: The ecosystem demography model (ED). *Ecological Monographs*, *71*(4), 557–586. https://doi.org/10.1890/0012-9615(2001)071(0557:AMFSVD)2.0.CO;2

Niinemets, Ü., Keenan, T. F., & Hallik, L. (2015). A worldwide analysis of within-canopy variations in leaf structural, chemical and physiological traits across plant functional types. *New Phytologist*, *205*(3), 973–993. https://doi.org/10.1111/nph.13096

Oleson, K., Lawrence, D., Bonan, G. B., Flanner, M., Kluzek, E., Lawrence, P., et al. (2010). Technical description of version 4.0 of the community land model (CLM), pp. 1-266, National Center for Atmospheric Research.

Oleson, K., Lawrence, D. M., Bonan, G. B., Drewniak, B., Huang, M., Koven, C. D., et al. (2013). Technical description of version 4.5 of the community land model (CLM), p. 420, NCAR Technical Note NCAR, Boulder.

Reich, P. B., Tjoelker, M. G., Pregitzer, K. S., Wright, I. J., Oleksyn, J., & Machado, J.-L. (2008). Scaling of respiration to nitrogen in leaves, stems and roots of higher land plants. *Ecology Letters*, *11*(8), 793–801. https://doi.org/10.1111/j.1461-0248.2008.01185.x

Reichstein, M., Bahn, M., Mahecha, M. D., Kattge, J., & Baldocchi, D. D. (2014). Linking plant and ecosystem functional biogeography. *Proceedings of the National Academy of Sciences*, *111*(38), 13,697–13,702. https://doi.org/10.1073/pnas.1216065111

Ryan, M. G. (1991). Effects of climate change on plant respiration. *Ecological Applications*, *1*(2), 157–167. https://doi.org/10.2307/1941808

Shaver, G. R., Bret-Harte, S. M., Jones, M. H., Johnstone, J., Gough, L., Laundre, J., & Chapin, F. S. (2001). Species composition interacts with fertilizer to control long-term change in tundra productivity. *Ecology*, *82*(11), 3163–3181. https://doi.org/10.1890/0012-9658(2001)082(3163:SCIWFT)2.0.CO;2

Smallman, T. L., & Williams, M. (2019). Description and validation of an intermediate complexity model for ecosystem photosynthesis and evapotranspiration: ACM-GPP-ETv1. *Geoscientific Model Development*, *12*, 2227–2253. https://doi.org/10.5194/gmd-12-2227-2019

Street, L. E., Shaver, G. R., Rastetter, E. B., Van Wijk, M. T., Kaye, B. A., & Williams, M. (2012). Incident radiation and the allocation of nitrogen within Arctic plant canopies: Implications for predicting gross primary productivity. *Global Change Biology*, *18*(9), 2838–2852. https://doi.org/10.1111/j.1365-2486.2012.02754.x

Van Wijk, M. T., Williams, M., & Shaver, G. R. (2005). Tight coupling between leaf area index and foliage N content in arctic plant communities. *Oecologia*, *142*(3), 421–427. https://doi.org/10.1007/s00442-004-1733-x

Waring, R. H., & Schlesinger, W. H. (1985). *Forest ecosystems: Concepts and management*. Orlando, FL: Academic Press.

Wehr, R., Munger, J. W., McManus, J. B., Nelson, D. D., Zahniser, M. S., Davidson, E. A., et al. (2016). Seasonality of temperate forest photosynthesis and daytime respiration. *Nature*, *534*(7609), 680–683. https://doi.org/10.1038/nature17966

Williams, M., Eugster, W., Rastetter, E. B., McFadden, J. P., & Chapin, F. S. III (2000). The controls on net ecosystem productivity along an arctic transect: A model comparison with flux measurements. *Global Change Biology*, *6*(suppl. 1), 116–126. https://doi.org/10.1046/j.1365-2486.2000.06016.x

Williams, M., Malhi, Y., Nobre, A., Rastetter, E. B., Grace, J., & Pereira, M. G. P. (1998). Seasonal variation in net carbon exchange and evapotranspiration in a Brazilian rain forest: A modelling analysis. *Plant, Cell and Environment*, *21*, 953–968. https://doi.org/10.1046/j.1365-3040.1998.00339.x

Williams, M., & Rastetter, E. B. (1999). Vegetation characteristics and primary productivity along an arctic transect: Implications for scaling-up. *Journal of Ecology*, *87*, 885–898. https://doi.org/10.1046/j.1365-2745.1999.00404.x

Williams, M., Rastetter, E. B., Fernandes, D. N., Goulden, M. L., Shaver, G. R., & Johnson, L. C. (1997). Predicting gross primary productivity in terrestrial ecosystems. *Ecological Applications*, *7*(3), 882–894. https://doi.org/10.1890/1051-0761(1997)007(0882:PGPPIT)2.0.CO;2

Williams, M., Rastetter, E. B., Fernandes, D. N., Goulden, M. L., Wofsy, S. C., Shaver, G. R., et al. (1996). Modelling the soil-plant-atmosphere continuum in a *Quercus-Acer* stand at Harvard Forest: The regulation of stomatal conductance by light, nitrogen and soil/plant hydraulic properties. *Plant, Cell and Environment*, *19*, 911–927. https://doi.org/10.1111/j.1365-3040.1996.tb00456

Wright, I. J., Reich, P. B., Westoby, M., Ackerly, D. D., Baruch, Z., Bongers, F., et al. (2004). The worldwide leaf economics spectrum. *Nature*, *428*(6985), 821–827. https://doi.org/10.1038/nature02403

Xu, X., Medvigy, D., Joseph Wright, S., Kitajima, K., Wu, J., Albert, L. P., et al. (2017). Variations of leaf longevity in tropical moist forests predicted by a trait-driven carbon optimality model. *Ecology Letters*, *20*(9), 1097–1106. https://doi.org/10.1111/ele.12804